

HETEROGENEOUS FLOW STRUCTURE IN GAS-SOLID RISERS: CONTINUOUS MODELING

Dawei Wang¹, Jun You¹, Chao Zhu^{1*}

1 New Jersey Institute of Technology, Newark, NJ 07102, USA

Abstract - Gas-solid riser flow exhibits strong heterogeneous structure in both axial direction and radial directions. Recent experimental studies reveal that the general radial solids concentration profiles present a double ring structure and the formation of a solid core region which have a relative higher concentration than the annulus region. This paper is focused on a comprehensive modeling of continuous gas-solids flow structure both in radial and axial directions. The specific transport mechanism due to collisional diffusive mass transfer and turbulent mass transfer are modeled. The radial heterogeneous flow structure of solids and gas at the different stage of the riser are investigated in detail. This mechanistic model, implemented with a detailed axial flow structure model, consists of a set of coupled ordinary-differential equations developed from conservation laws of mass, momentum and kinetic energy of both gas and solids phases. The solving algorithm is based on the Runge-Kutta method. The proposed model predicts the phase transport profiles such as the solids concentration, phase velocities and pressure drops in different regions along the riser. The model also yields the critical information of flow structure characteristics such as back flow, wall frictions and choking.

INTRODUCTION

Recent measurement of circulating fluidized bed riser with Electrical Capacitance Tomography (ECT) reveals a double ring structure of solids concentration and a solids core region flow structure in radial direction (Du et al. (2004)). This double ring structure appears to be stable along the riser, and could be observed under a wide range of CFB operation conditions.

Most models on heterogeneous flow structure are based on the core-annulus (wall) flows (Bolton and Davidson, (1988); Rhodes and Geldart, (1987); Horio et al, (1988); Senior and Brereton, (1992)), which typically consider a dilute uniform core flow, and a dense wall flow along the riser. Most of these models ignore the detailed mechanisms in the bottom region of riser where the flows can be very dense and complex. A primitive model was lately proposed to interpret the reported core-annulus-wall structure (Zhu et al., (2005)), using a simplified kinetic theory model to account for the solids acceleration in collision dominated dense flow regimes near the bottom of riser. It is realized, however, that most traditional momentum-based models with the assistance of kinetic theory modeling approach may be insufficient to describe some basic physics of collision-induced energy dissipation in fluidization, such as energy dissipations from tangential slip and rotational slip. This deficiency may be represented by the inability of correctly predicting the pressure distribution in the dense flow regime near the bottom of a CFB riser. The importance of correct account of energy transport and dissipation in the momentum equation may be analogous to that of $k-\epsilon$ model in the turbulent momentum transport equations in turbulence flows. Hence an additional term due to energy dissipation should be introduced in solid momentum transport equation in the collision and acceleration dominated regime (Zhu and You, (2006)).

A 3-zone model is recently presented to simulate the heterogeneous structure of the riser flow (Zhu et al. (2007)). The model yields a reasonable explanation not only for “core-annulus (wall)” flow structure but also the “core-annulus-wall” flow structure in riser flows. While, the model artificially divides the riser into 3 different zones and uses averaged values to describe the characteristics of the flow in each zone, thus it can not reveal the intrinsic mechanism and relationship of solids mass transport of each place. To make the problem to be closed, the model uses the pre-defined wall zone conditions to simulate the structure in core and annulus zones.

This paper is aimed to present a continuous modeling approach with intrinsic mass transfer mechanism to characterize the formation mechanisms of heterogeneous structure in a CFB riser.

* corresponding author: zhu@adm.njit.edu

GENERAL GOVERNING EQUATIONS

Basically, the flow in a riser could be described with following governing equations based on the mass and momentum conservation of each phase.

$$\frac{d}{dz} \left(\int_A \alpha_g \rho_g U_g dA \right) = 0 \quad (1)$$

$$\frac{d}{dz} \left(\int_A \alpha_s \rho_s U_s dA \right) = 0 \quad (2)$$

$$-\frac{d \left(\int_A P dA \right)}{dz} = \tau_w l_w + \int_A \alpha_g \rho_g g dA + \frac{d \left(\int_A \alpha_g \rho_g U_g^2 dA \right)}{dz} + \int_A F_D dA \quad (3)$$

$$\frac{d \left(\int_A \alpha_s \rho_s U_s^2 dA \right)}{dz} = \int_A F_D dA - \tau_{sw} l_{sw} - \int_A \alpha_s \rho_s g dA - \int_A F_C dA \quad (4)$$

With the volumetric fraction relations of gas and solids phase and the equation of state of gas phase:

$$\alpha_g + \alpha_s = 1 \text{ and } \rho_g = \frac{P}{RT}.$$

Where, F_D is the drag force which is given by Richard-Zaki equation (Richardson and Zaki (1954)),

$$F_D = \frac{18\mu}{d_s^2} \frac{\alpha_s}{(1-\alpha_s)^L} \cdot (U_g - U_s) \quad (5)$$

F_C is the solid momentum transport due to energy dissipation in the dense and acceleration region (Zhu and You (2006)) which is

$$F_C = -\frac{\Gamma - (U_g - U_s) \left(-\frac{dP}{dz} \right)}{U_s} \quad (6)$$

Where, Γ represents the energy dissipations due to inter-phase frictional and inter-particle collision.

$$\Gamma \approx \sum_{j=0}^N k_j \alpha_s^j \quad (7)$$

τ_w and τ_{sw} are respectively the friction stresses between the wall and the gas phase and the solids phase.

For radically uniform flow, the integrals in above equation could be replaced by an averaged value; the closure of the problem for axially heterogeneous flow structure is fulfilled

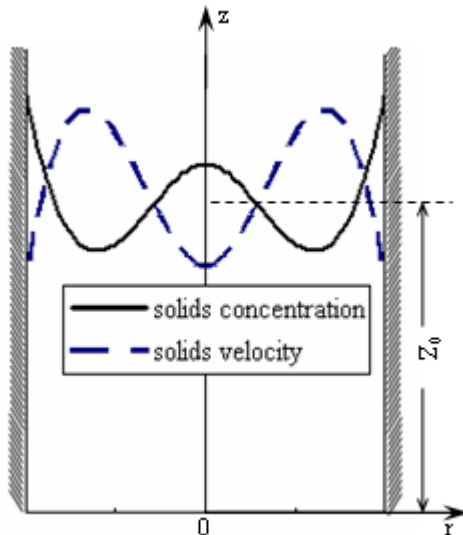


Figure 1. Representative flow structure by term of 3rd order polynomials

For the heterogeneous flow structure in both radial and axial directions, we assume that the transport parameters ϕ could be expressed as polynomials with following form:

$$\phi(r, z) = \sum_{i=0}^n c_{\phi i}(z) \cdot r^i.$$

We use 3rd order polynomials to approximate the distribution,

$$\phi(r, z) = c_{\phi 3}(z)r^3 + c_{\phi 2}(z)r^2 + c_{\phi 1}(z)r + c_{\phi 0}(z) \quad (8)$$

Here, ϕ could be $\alpha_s(r, z)$, $U_s(r, z)$ or $U_g(r, z)$.

It is noted that the pressure distribution at an arbitrary cross-section is uniform. That means the gas density is constant at a cross-section.

The coefficients of $C_{\phi i}$ could be given by

$c_{\phi 0} = \phi_0(z)$ is the value of $\phi(r, z)$ at the center line;

$c_{\phi 1} = 0$ from axi-symmetry of the riser;

$$c_{\phi 2} = \frac{3(\phi_w(z) - \phi_0(z)) - \delta_{\phi_w}(z)R}{R^2}; \quad c_{\phi 3} = \frac{\delta_{\phi_w}(z)R - 2(\phi_w(z) - \phi_0(z))}{R^3}$$

Where, $\phi_w(z)$ is the value of $\phi(r, z)$ at the wall, and $\delta_{\phi_w}(z)$ is the radial gradient of $\phi(r, z)$ at the wall.

Where, $\phi_w(z)$ is the value of $\phi(r, z)$ at the wall, and $\delta_{\phi_w}(z)$ is the radial gradient of $\phi(r, z)$ at the wall.

Put the polynomials of solids concentration, solids velocity and gas velocity with above form into governing equation (1)-(4), and with the truth that the pressure across any cross-section of the riser is uniform, we could have

$$\begin{bmatrix} C_{1,1} & C_{1,2} & C_{1,3} & C_{1,4} & C_{1,5} & C_{1,6} & C_{1,7} & C_{1,8} & C_{1,9} & C_{1,10} \\ C_{2,1} & C_{2,2} & C_{2,3} & C_{2,4} & C_{2,5} & C_{2,6} & C_{2,7} & C_{2,8} & C_{2,9} & C_{2,10} \\ C_{3,1} & C_{3,2} & C_{3,3} & C_{3,4} & C_{3,5} & C_{3,6} & C_{3,7} & C_{3,8} & C_{3,9} & C_{3,10} \\ C_{4,1} & C_{4,2} & C_{4,3} & C_{4,4} & C_{4,5} & C_{4,6} & C_{4,7} & C_{4,8} & C_{4,9} & C_{4,10} \end{bmatrix} \begin{pmatrix} \frac{d\alpha_{s0}}{dz} \\ \frac{d\alpha_{sw}}{dz} \\ \frac{d\delta_{\alpha sw}}{dz} \\ \frac{dU_{g0}}{dz} \\ \frac{dU_{gw}}{dz} \\ \frac{d\delta_{ugw}}{dz} \\ \frac{dU_{s0}}{dz} \\ \frac{dU_{sw}}{dz} \\ \frac{d\delta_{usw}}{dz} \\ \frac{dP}{dz} \end{pmatrix} = \begin{pmatrix} 0 \\ 0 \\ -\frac{\int F_D dA + \tau_w l_w}{A} \\ \frac{\int_A (1 - \lambda_c) F_D dA - \tau_{ws} l_{ws}}{A} \end{pmatrix} \quad (\text{Group A})$$

Where C_{ij} are coefficients explicitly expressed by terms of α_{s0} , α_{sw} , $\delta_{\alpha sw}$, U_{g0} , U_{gw} , δ_{ugw} , U_{s0} , U_{sw} and δ_{usw} . (see appendix A)

we have ten unknowns (α_{s0} , α_{sw} , $\delta_{\alpha sw}$, U_{s0} , U_{sw} , δ_{usw} , U_{g0} , U_{gw} , δ_{ugw} , P), and we have only 4 governing equations ((8)-(11)). These 4 governing equations describe the axial heterogeneous flow structure along the riser and could only be used to represent the change of averaged flow structure parameters $\bar{\alpha}_s, \bar{U}_g, \bar{U}_s$.

To closure the problem of heterogeneous flow structure (in both radial and axial directions), 6 additional intrinsic correlations (in radial direction) are needed. These 6 correlations will quantify the radial transport of phases in terms of $\phi_0(z), \phi_w(z), \delta_{w\phi}(z)$, which link the transport properties of centerline to those at the wall and shall cover the flow structure of concentrations and velocities of both gas and solids phases across any cross-section of the riser. They shall reveal the radial mass transport caused by the turbulence and collisional diffusion as well as the effect of wall boundary constraint on the flow structure.

INTRINSIC MECHANISM AND PROBLEM CLOSURE

Based on the non-slip condition of gas phase at the wall boundary, the gas velocity at the wall shall be zero. We have $U_{gw}(z) = 0$. We also assume that the friction between the gas phase and the wall is small enough and could be neglected, thus the radial change rate of gas velocity at the wall could be assumed to be zero.

We could write $\delta_{U_{gw}}(z) = 0$. The above two equations along with the averaged gas velocity given by the previous governing equation could give the gas velocity distribution across the cross-section of riser which is characterized with three characteristic values $U_{g0}(z)$, $U_{gw}(z)$, $\delta_{ugw}(z)$.

For the solids volume fraction, we could also assume it is packed on the wall and thus is the constant value, which gives

$$\alpha_{sw}(z) = \alpha_{packed} = \text{constant} \quad (9)$$

Based on the force balance of solids phase at the wall, we could have

$$F_{Dw} - \frac{\partial \tau_{sw}}{\partial r} l_{sw} - \rho_s \alpha_s g = \alpha_s \rho_s \frac{dU_{sw}}{dz} \quad (10)$$

Where, F_{Dw} is the drag force of gas phase on the solids phase at the wall.

The formation mechanism of radial heterogeneous flow structure is the radial solids transport due to the turbulent mass transfer and collisional diffusive mass transfer of solids particles. The intensity of turbulent mass transfer is dependent on the local turbulent intensity and the velocity gradient of solids and is from high velocity to low velocity. The intensity of mass transfer is dependent on the local solids concentration and the concentration gradient of solids phase, the direction is from high concentration to low concentration. The net value of these two mass transfers gives the local solids transport. $J_{net} = J_{T.C.} + J_{C.D.}$.

Based on the mass conservation of solids phase, the total mass flow of solids phase across the cross-section shall keep unchanged although the solids may transfer inwards or outwards locally, and we could write:

$$\int \frac{\partial J_{net}}{\partial r} dA = 0 \quad (11)$$

Where, For the simplicity of the problem, we assume the coefficients of turbulent convective and collisional diffusive mass transfers are respectively proportional to the local velocity and solids concentration.

$$J_{TC} = -D_{turb} U_s \rho_s \frac{\partial U_s}{\partial r}; \quad J_{CD} = -D_{diff} \alpha_s \rho_s \frac{\partial \alpha_s}{\partial r}$$

The radial transport of solids also causes the radial solids momentum shift, which is balanced by the radial stress of the wall boundary and represented as the form of solids pressure. We assume that the solids pressure is equal to the gravity of the solids phase at each height.

$$\int J_{net} U_s dA = \sigma_{sw} \quad (12)$$

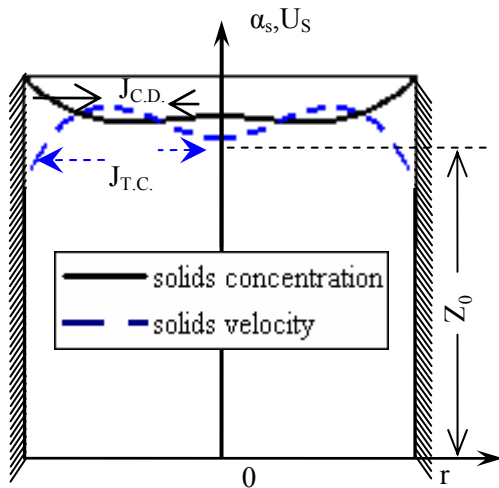
With above equations of intrinsic mechanism and simplifications, we could obtain 7 independent equations (equation group A and 10-12) for 7 variables (α_{s0} , δ_{asw} , U_{s0} , U_{sw} , δ_{usw} , U_{g0} , P) to describe the heterogeneous flow structure in a riser. They are given as:

$$\begin{bmatrix} D_{1,1} & D_{1,2} & D_{1,3} & D_{1,4} & D_{1,5} & D_{1,6} & D_{1,7} \\ D_{2,1} & D_{2,2} & D_{2,3} & D_{2,4} & D_{2,5} & D_{2,6} & D_{2,7} \\ D_{3,1} & D_{3,2} & D_{3,3} & D_{3,4} & D_{3,5} & D_{3,6} & D_{3,7} \\ D_{4,1} & D_{4,2} & D_{4,3} & D_{4,4} & D_{4,5} & D_{4,6} & D_{4,7} \\ D_{5,1} & D_{5,2} & D_{5,3} & D_{5,4} & D_{5,5} & D_{5,6} & D_{5,7} \\ D_{6,1} & D_{6,2} & D_{6,3} & D_{6,4} & D_{6,5} & D_{6,6} & D_{6,7} \\ D_{7,1} & D_{7,2} & D_{7,3} & D_{7,4} & D_{7,5} & D_{7,6} & D_{7,7} \end{bmatrix} \begin{pmatrix} \frac{d\alpha_{s0}}{dz} \\ \frac{d\delta_{asw}}{dz} \\ \frac{dU_{g0}}{dz} \\ \frac{dU_{s0}}{dz} \\ \frac{dU_{sw}}{dz} \\ \frac{d\delta_{usw}}{dz} \\ \frac{dP}{dz} \end{pmatrix} = \begin{pmatrix} 0 \\ 0 \\ -\frac{\int F_D dA + \tau_w l_w}{A} \\ \frac{\int_A (1 - \lambda_c) F_D dA - \tau_{ws} l_{ws}}{A} \end{pmatrix} \quad (\text{Group B})$$

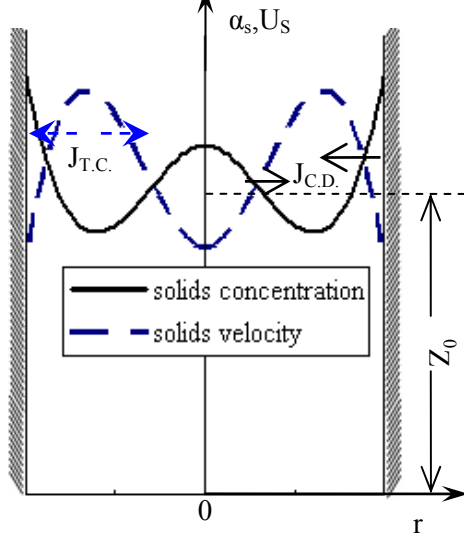
Where D_{ij} are coefficients explicitly expressed by terms of α_{s0} , δ_{asw} , U_{g0} , U_{s0} , U_{sw} and δ_{usw} . (see appendix B).

The closure of the problem is obtained.

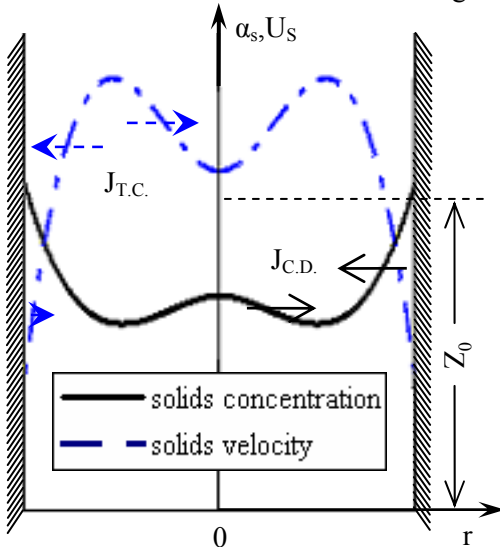
EXPECTED RESULTS AND DISCUSSIONS



(a) solids concentration and velocity distribution at riser inlet



(a) solids concentration and velocity distribution at middle of riser height



(a) solids concentration and velocity distribution at middle of riser height

To preliminarily evaluate the correctness of our model, some analysis and discussion are made. We assume that at the inlet of the riser, the solids concentration and solids velocity are slightly non-uniform across the cross-section as shown in figure 2(a). The directions of the solids mass transfers due to turbulence and collisional diffusion are also shown. Figure 2(b) shows the net mass transport of solids phase. The solids always transport outwards from the inner of the riser across the cross-section, which could make the flow structure more non-uniform. As the transport amount in the middle part of the riser is higher than that in the center part, the middle part shall become dilute much faster than the center part.

After the process of solids acceleration, the solids velocities in the middle and center regions increase while the velocity at the wall boundary shall decrease due to the wall friction. The non-uniformity of the radial flow structure becomes higher (figure 3(a)). Now, the direction of net mass transport would be from the outer side into the inner side of the riser (figure 3(b)).

With further radial mass transport of solids and development of flow structure, the solids velocity and concentration distributions change further as shown in figure 4(a). The solids concentrations of core and annulus zone are very dilute, while the concentration in the core zone is still higher than that of annulus zone. Due to the friction of the wall, the solids velocity at the wall boundary decreases further and becomes to move downwards. Now, the solids transport radially from inner side to outer side of the riser.

CONCLUSIONS

This paper presents a complete mechanistic model to interpret the heterogeneous flow structure in riser flows. The governing equations of mass and momentum conservation of gas and solids phases are given to describe the axial flow structure. The intrinsic mechanism of radial mass transport is presented to reveal the formation process of the radial heterogeneous flow structure. The proposed mechanism yields a reasonable explanation for the heterogeneous riser flow structure in both radial and axial directions. Typical radial distributions of solids velocity and concentration at different stage of riser flow are described and analyzed. More quantitative comparison and investigation of parametric study could be conducted in future studies.

NOTATION

α_g	gas volume fraction	p	pressure, Pa
U_g	gas velocity, m/s	$L_{\mu m}$	length, m
A	area, m^2	p_{ref}	reference pressure at cyclone exit, Pa
z	riser height, m		overall riser pressure drop, Pa
ρ_g	gas density, kg/m^3	R	diameter of the riser, m
α_s	solids volume fraction	t	time, s
U_s	solids velocity, m/s	u	superficial gas velocity, m/s
ρ_s	solids density, kg/m^3	U	signal of fiber-optical probes, V
F_D	drag force, N/m^3	U_0	signal of fiber-optical probes for $c_v = 0$, V
g	gravity constant, m/s^2	ε	voidage, -
H_b	height of the bottom zone, m	$\bar{\varepsilon}$	cross-sectional average voidage, -
j	exponent defined by eq. 2, -	P	Pressure, Pa
k	exponent defined by eq. 2, -		
r	radial position, m		

REFERENCES

- Du, B., W. Warsito and L.-S. Fan, "ECT studies of the choking phenomenon in a gas-solid circulating fluidized bed", *AICHE J.*, 50 (7), 1386 (2004).
- Bolton, L.W. and Davidson, J.F.(1988). Recirculation of Particles in Fast Fluidized Risers. In *Circulation Fluidized Bed Technology* _ Ed. Basu and Large. Toronto: Pergamon Press
- Rhodes, M.J. and Geldart, D. (1987). A Model for the Circulating Fluidized Bed. *Powder Tech.*, 53, 155
- Horio, M., Morishita, K., Tachibana, O. and Murata, N. (1988). Solid Distribution and Movement in Circulating Fluidized Beds. In *Circulating Fluidized Bed Technology* _ Ed. Basu and Large. Toronto: Pergamon Press
- Senior, R.C. and Brereton, C.M.M. (1992). Modeling of Circulating Fluidized Bed Solids Flow and Distribution. *Chem. Eng. Sci.*, 47, 281.
- Zhu, C., Yu, Q., and L.S.Fan, Modeling on Core-annulus-wall Structure in Circulating Fluidized Bed Riser, *Circulating Fluidized Bed Technology* _ , 354, 2005
- Zhu, C. and You, J. An Energy-Based Model of Gas-Solids Transport in a Riser, *Powder Tech.*, 2006
- Chao Zhu, Jun You, Dawei Wang, Liang-Shih Fan, Modeling on Heterogeneous Structure in Acceleration Regime of Gas-Solid Riser Flows, *Fluidization XII*, 119
- Rhodes, M.J., M. Sollaart and X.S. Wang, "Flow structure in a fast fluid bed", *Powder Technology*, 99, 194 (1998).
- Richardson, J.F., Zaki, W.N., Sedimentation and fluidization, *Trans. Inst. Chem. Eng.*, vol. 32: p. 35-53. (1954)

APPENDIX A

$$\text{Where } \left\{ \begin{array}{l} D_1 = \frac{\delta_{\alpha_{gw}} R^2}{168} - \frac{\alpha_{gw} R}{28} - \frac{\alpha_{g0} R}{28} \\ D_2 = \frac{\delta_{ugw} R^2}{168} - \frac{U_{gw} R}{28} - \frac{U_{g0} R}{28} \\ D_3 = \frac{2\alpha_{gw}}{7} + \frac{9\alpha_{g0}}{140} - \frac{\delta_{\alpha_{gw}} R}{28} \\ D_4 = \frac{2U_{gw}}{7} + \frac{9U_{g0}}{140} - \frac{\delta_{ugw} R}{28} \\ D_5 = \frac{9\alpha_{gw}}{140} + \frac{3\alpha_{g0}}{35} - \frac{\delta_{\alpha_{gw}} R}{70} \\ D_6 = \frac{9U_{gw}}{140} + \frac{3U_{g0}}{35} - \frac{\delta_{ugw} R}{70} \end{array} \right. \quad \text{and} \quad \left\{ \begin{array}{l} D_7 = \frac{\delta_{\alpha_{sw}} R^2}{168} - \frac{\alpha_{sw} R}{28} - \frac{\alpha_{s0} R}{28} \\ D_8 = \frac{\delta_{usw} R^2}{168} - \frac{U_{sw} R}{28} - \frac{U_{s0} R}{28} \\ D_9 = \frac{2\alpha_{sw}}{7} + \frac{9\alpha_{s0}}{140} - \frac{\delta_{\alpha_{sw}} R}{28} \\ D_{10} = \frac{2U_{sw}}{7} + \frac{9U_{s0}}{140} - \frac{\delta_{usw} R}{28} \\ D_{11} = \frac{9\alpha_{sw}}{140} + \frac{3\alpha_{s0}}{35} - \frac{\delta_{\alpha_{sw}} R}{70} \\ D_{12} = \frac{9U_{sw}}{140} + \frac{3U_{s0}}{35} - \frac{\delta_{usw} R}{70} \end{array} \right.$$

$$\text{and} \quad \left\{ \begin{array}{l} D_{\delta_{1w}} = I_1 \delta_{2w}^2 R^3 + I_2 \phi_{2w} \delta_{2w} R^2 + I_3 \phi_{20} \delta_{2w} R^2 + I_4 \phi_{2w}^2 R + I_5 \phi_{20} \phi_{2w} R + I_6 \phi_{20}^2 R \\ D_{\phi_{1w}} = I_7 \delta_{2w}^2 R^2 + I_8 \phi_{2w} \delta_{2w} R + I_9 \phi_{20} \delta_{2w} R + I_{10} \phi_{2w}^2 + I_{11} \phi_{20} \phi_{2w} + I_{12} \phi_{20}^2 \\ D_{\phi_{10}} = I_{13} \delta_{2w}^2 R^2 + I_{14} \phi_{2w} \delta_{2w} R + I_{15} \phi_{20} \delta_{2w} R + I_{16} \phi_{2w}^2 + I_{17} \phi_{20} \phi_{2w} + I_{18} \phi_{20}^2 \\ D_{\delta_{2w}} = 2I_1 \delta_{1w} \delta_{2w} R^3 + I_2 \delta_{1w} \phi_{2w} R^2 + I_3 \delta_{1w} \phi_{20} R^2 + 2I_7 \phi_{1w} \delta_{2w} R^2 + I_8 \phi_{1w} \phi_{2w} R + I_9 \phi_{1w} \phi_{20} R + 2I_{13} \phi_{10} \delta_{2w} R^2 + I_{14} \phi_{1w} \phi_{2w} R + I_{15} \phi_{10} \phi_{20} R \\ D_{\phi_{2w}} = I_2 \delta_{1w} \delta_{2w} R^2 + 2I_4 \delta_{1w} \phi_{2w} R + I_5 \delta_{1w} \phi_{20} R + I_8 \phi_{1w} \delta_{2w} R + 2I_{10} \phi_{1w} \phi_{2w} + I_{11} \phi_{1w} \phi_{20} + I_{14} \phi_{10} \delta_{2w} R + 2I_{16} \phi_{10} \phi_{2w} + I_{17} \phi_{10} \phi_{20} \\ D_{\phi_{20}} = I_3 \delta_{1w} \delta_{2w} R^2 + I_5 \delta_{1w} \phi_{2w} R + 2I_6 \delta_{1w} \phi_{20} R + I_9 \phi_{1w} \delta_{2w} R + I_{11} \phi_{1w} \phi_{2w} + 2I_{12} \phi_{1w} \phi_{20} + I_{15} \phi_{10} \delta_{2w} R + I_{17} \phi_{10} \phi_{2w} + 2I_{18} \phi_{10} \phi_{20} \end{array} \right.$$

APPENDIX B

$$D_1 \frac{d\delta_{ugw}}{dz} + D_2 \frac{d\delta_{\alpha g}}{dz} + D_3 \frac{dU_{gw}}{dz} + D_4 \frac{d\alpha_{gw}}{dz} + D_5 \frac{dU_{g0}}{dz} + D_6 \frac{d\alpha_{g0}}{dz} = 0 \quad (9)$$

$$D_7 \frac{d\delta_{usw}}{dz} + D_8 \frac{d\delta_{\alpha s}}{dz} + D_9 \frac{dU_{sw}}{dz} + D_{10} \frac{d\alpha_{sw}}{dz} + D_{11} \frac{dU_{s0}}{dz} + D_{12} \frac{d\alpha_{s0}}{dz} = 0 \quad (10)$$

$$\frac{dP}{dz} = \frac{\tau_{ws}}{A} + \frac{\int F_D dA}{A} + (2D_{\delta\alpha g} - \frac{\rho_g g R}{10}) \frac{d\delta_{\alpha gw}}{dz} + (2D_{\alpha gw} + \frac{7\rho_g g}{10}) \frac{d\alpha_{gw}}{dz} + (2D_{\alpha g0} + \frac{3\rho_g g}{10}) \frac{d\alpha_{g0}}{dz} + 2D_{\delta ug} \frac{d\delta_{ugw}}{dz} + 2D_{ugw} \frac{dU_{gw}}{dz} + 2D_{ug0} \frac{dU_{g0}}{dz} \quad (11)$$

$$(2D_{\alpha s} - \frac{\rho_s g R}{10}) \frac{d\delta_{\alpha sw}}{dz} + (2D_{\alpha sw} + \frac{7\rho_s g}{10}) \frac{d\alpha_{sw}}{dz} + (2D_{\alpha s0} + \frac{3\rho_s g}{10}) \frac{d\alpha_{s0}}{dz} + 2D_{\delta us} \frac{d\delta_{usw}}{dz} + 2D_{usw} \frac{dU_{sw}}{dz} + 2D_{us0} \frac{dU_{s0}}{dz} = \frac{\int_A (1-\lambda_c) F_D dA - \tau_{ws} I_{ws}}{A} \quad (12)$$

$$\text{Where } \left\{ \begin{array}{l} D_1 = \frac{\delta_{\alpha gw} R^2}{168} - \frac{\alpha_{gw} R}{28} - \frac{\alpha_{g0} R}{28} \\ D_2 = \frac{\delta_{ugw} R^2}{168} - \frac{U_{gw} R}{28} - \frac{U_{g0} R}{28} \\ D_3 = \frac{2\alpha_{gw}}{7} + \frac{9\alpha_{g0}}{140} - \frac{\delta_{\alpha gw} R}{28} \\ D_4 = \frac{2U_{gw}}{7} + \frac{9U_{g0}}{140} - \frac{\delta_{ugw} R}{28} \\ D_5 = \frac{9\alpha_{gw}}{140} + \frac{3\alpha_{g0}}{35} - \frac{\delta_{\alpha gw} R}{70} \\ D_6 = \frac{9U_{gw}}{140} + \frac{3U_{g0}}{35} - \frac{\delta_{ugw} R}{70} \end{array} \right. \quad \text{and} \quad \left\{ \begin{array}{l} D_7 = \frac{\delta_{\alpha sw} R^2}{168} - \frac{\alpha_{sw} R}{28} - \frac{\alpha_{s0} R}{28} \\ D_8 = \frac{\delta_{usw} R^2}{168} - \frac{U_{sw} R}{28} - \frac{U_{s0} R}{28} \\ D_9 = \frac{2\alpha_{sw}}{7} + \frac{9\alpha_{s0}}{140} - \frac{\delta_{\alpha sw} R}{28} \\ D_{10} = \frac{2U_{sw}}{7} + \frac{9U_{s0}}{140} - \frac{\delta_{usw} R}{28} \\ D_{11} = \frac{9\alpha_{sw}}{140} + \frac{3\alpha_{s0}}{35} - \frac{\delta_{\alpha sw} R}{70} \\ D_{12} = \frac{9U_{sw}}{140} + \frac{3U_{s0}}{35} - \frac{\delta_{usw} R}{70} \end{array} \right.$$

$$\text{and} \quad \left\{ \begin{array}{l} D_{\delta 1w} = I_1 \delta_{2w}^2 R^3 + I_2 \phi_{2w} \delta_{2w} R^2 + I_3 \phi_{2w} \delta_{2w} R^2 + I_4 \phi_{2w}^2 R + I_5 \phi_{2w} \phi_{2w} R + I_6 \phi_{2w}^2 R \\ D_{\phi 1w} = I_7 \delta_{2w}^2 R^2 + I_8 \phi_{2w} \delta_{2w} R + I_9 \phi_{2w} \delta_{2w} R + I_{10} \phi_{2w}^2 + I_{11} \phi_{2w} \phi_{2w} + I_{12} \phi_{2w}^2 \\ D_{\phi 10} = I_{13} \delta_{2w}^2 R^2 + I_{14} \phi_{2w} \delta_{2w} R + I_{15} \phi_{2w} \delta_{2w} R + I_{16} \phi_{2w}^2 + I_{17} \phi_{2w} \phi_{2w} + I_{18} \phi_{2w}^2 \\ D_{\delta 2w} = 2I_1 \delta_{1w} \delta_{2w} R^3 + I_2 \delta_{1w} \phi_{2w} R^2 + I_3 \delta_{1w} \phi_{2w} R^2 + 2I_4 \phi_{1w} \delta_{2w} R^2 + I_5 \phi_{1w} \phi_{2w} R + I_6 \phi_{1w} \phi_{2w} R + 2I_{13} \phi_{10} \delta_{2w} R^2 + I_{14} \phi_{1w} \phi_{2w} R + I_{15} \phi_{10} \phi_{2w} R \\ D_{\phi 2w} = I_2 \delta_{1w} \delta_{2w} R^2 + 2I_4 \delta_{1w} \phi_{2w} R + I_5 \delta_{1w} \phi_{2w} R + I_8 \phi_{1w} \delta_{2w} R + 2I_{10} \phi_{1w} \phi_{2w} + I_{11} \phi_{1w} \phi_{2w} + I_{14} \phi_{10} \delta_{2w} R + 2I_{16} \phi_{10} \phi_{2w} + I_{17} \phi_{10} \phi_{2w} \\ D_{\phi 20} = I_3 \delta_{1w} \delta_{2w} R^2 + I_5 \delta_{1w} \phi_{2w} R + 2I_6 \delta_{1w} \phi_{2w} R + I_9 \phi_{1w} \delta_{2w} R + I_{11} \phi_{1w} \phi_{2w} + 2I_{12} \phi_{1w} \phi_{2w} + I_{15} \phi_{10} \delta_{2w} R + I_{17} \phi_{10} \phi_{2w} + 2I_{18} \phi_{10} \phi_{2w} \end{array} \right.$$